Molecular Physics

Analysis of highly excited 'hot' bands in the SO_2 molecule: $\nu_2 + 3\nu_3 - \nu_2$ and $2\nu_1 + \nu_2 + \nu_3 - \nu_2$

O. N. Ulenikov[a]; E. S. Bekhtereva[a]; O. V. Gromova[a]; S. Alanko[b]; V. -M. Horneman[b]; C. Leroy[c]

[a] Laboratory of Molecular Spectroscopy, Physics Department, Tomsk State University, Tomsk, 634050, Russia [b] Department of Physics, University of Oulu, FIN-90014, Finland [c] Institut Carnot de Bourgogne-UMR 5209 CNRS, Université de Bourgogne, F-21078 Dijon Cedex, France

First published on: 27 January 2010

PLEASE SCROLL DOWN FOR ARTICLE

Taylor & Francis
Taylor & Francis Group

RESEARCH ARTICLE

Analysis of highly excited 'hot' bands in the SO_2 molecule: $v_2 + 3v_3 − v_2$ and $2v_1 + v_2 + v_3 − v_2$

O.N. Ulenikov[a]*, E.S. Bekhtereva[a], O.V. Gromova[a], S. Alanko[b], V.-M. Horneman[b] and C. Leroy[c]

[a]*Laboratory of Molecular Spectroscopy, Physics Department, Tomsk State University, Tomsk, 634050, Russia;*
[b]*Department of Physics, University of Oulu, P.O. Box 3000, FIN-90014, Finland;* [c]*Institut Carnot de Bourgogne-UMR 5209 CNRS, Université de Bourgogne B.P. 47870, F-21078 Dijon Cedex, France*

We set up a variational procedure of assignments of transitions and we applied it to the analysis very weak 'hot' bands, $v_2 + 3v_3 − v_2$ and $2v_1 + v_2 + v_3 − v_2$, of the SO_2 molecule. As the first step of the study, the 'cold' bands, $3v_3$ and $2v_1 + v_3$, are re-analysed and transitions belonging to those bands are assigned up to the values of quantum numbers $J^{max.} = 60$, $K_a^{max.} = 19$, and $J^{max.} = 69$, $K_a^{max.} = 20$ for the bands $3v_3$ and $2v_1 + v_3$, respectively. After 'cleaning' the experimental spectrum from transitions belonging to the $3v_3$ and $2v_1 + v_3$ bands, a variational procedure was used that allowed us to assign 230 and 115 transitions with the values of quantum numbers $J^{max.} = 35$, $K_a^{max.} = 10$, and $J^{max.} = 26$, $K_a^{max.} = 11$ for the bands $v_2 + 3v_3 − v_2$ and $2v_1 + v_2 + v_3 − v_2$, respectively. The sets of spectroscopic parameters obtained by fitting the assigned experimental transitions reproduce the initial experimental data with an accuracy close to experimental uncertainties.

Keywords: sulphur dioxide; high-resolution spectra; spectroscopic parameters

1. Introduction

High resolution ro-vibrational spectra of molecules is an unique source of information about internal dynamics, physical-chemical properties, and understanding the ways of chemical reactions. In this case, the higher the studied bands of a molecule, the more fundamental physical information can be extracted from experimentally recorded spectra. In the present communication we present the results of the first study of the ro-vibrational structure of two highly excited vibrational states, (013) and (211), of the SO_2 molecule.

The sulphur dioxide molecule is an important chemical species in many fields such as chemistry, astrophysics, atmospheric optics, laser techniques, etc. (see, e.g. the reviews in [1,2]). Thus, its spectra have been a subject of intense study for a long time (see the review in [3] and also [4–36]). However, up to now only the lowest vibrational bands of SO_2 have been analysed with high resolution. In particular, there are only a few publications where the states corresponding to more than three excitations of vibrational quanta have been discussed: the band $v_1 + 3v_2$ was analysed in [27], and the state (131) was considered in [26]. Additionally, the bands $v_1 + 3v_3$ and $3v_1 + v_3$ were discussed recently in [37].

In this paper we follow up on our recent studies, [36,37], of the highly excited vibrational states of the SO_2 molecule and discuss, for the first time, the ro-vibrational structures of two states, (013) and (211), on the basis of the assignment of transitions in two very weak hot bands, $v_2 + 3v_3 − v_2$ and $2v_1 + v_2 + v_3 − v_2$. Section 2 describes the experimental conditions for recording the spectra. In Section 3 we briefly present the Hamiltonian model used to fit of experimental line positions. The results of the re-analysis of the considerably stronger 'cold' bands $3v_3$ and $2v_1 + v_3$, that are located in the same region as the 'hot' bands, $v_2 + 3v_3 − v_2$ and $2v_1 + v_2 + v_3 − v_2$, are presented in Section 4. Section 5 is devoted to the analysis of these hot bands.

2. Experimental details

The analysis is based on two measurements around $3600\,cm^{-1}$ (Am) and above $4000\,cm^{-1}$ (Bm). The measured range was optically limited with interference filters. The experimental work was performed in the Infrared laboratory of Oulu using a Bruker IFS-120 HR Fourier spectrometer. The amount of carbon dioxide (CO_2) in the SO_2 sample, made by Sigma-Aldrich Inc.

---

*Corresponding author. Email: ulenikov@mail.ru

was reduced with cold traps before evaporating the sample into the multipath path White cell [38]. The sample pressure was 631 and 837 Pa in the Am and Bm measurements, respectively. The absorption path length was 153.6 m in both recordings. The cell was provided with two 6 mm thick potassium bromide windows. A tungsten source, a quartz beamsplitter and an indium antimonide semiconductor detector were used. The final spectral resolution limited by the instrumental resolution and Doppler and pressure broadening is between 0.0075 and 0.009 cm^{-1}. The measurements of these weak spectra required rather long recording times. The Am and Bm measurements were recorded in 85.6 and 48.7 h, respectively. The Am and Bm spectra were calibrated with 43 and with 19 water peaks, respectively [39], and the peak positions were calculated with the optimised centre of gravity method [40].

3. Hamiltonian model

The effective Hamiltonian of the XY_2-type molecule of the C_{2v} symmetry has been discussed in the spectroscopic literature many times. For consistency, we will briefly present it here without detailed explanations:

$$H^{\text{vib.-rot.}} = \sum_{v,\tilde{v}} |v\rangle\langle\tilde{v}|H^{v\tilde{v}}, \tag{1}$$

where v and $\tilde{v}$ denote possible interacting vibrational states. In this model the diagonal block operators are the traditional Watson type operators in A reduction and I^r representation [41],

$$
\begin{aligned}
H^{vv} &= E^v + \left[A^v - \frac{1}{2}(B^v + C^v)\right]J_z^2 + \frac{1}{2}(B^v + C^v)J^2 \\
&\quad + \frac{1}{2}(B^v - C^v)J_{xy}^2 - \Delta_K^v J_z^4 - \Delta_{JK}^v J_z^2 J^2 - \Delta_J^v J^4 \\
&\quad - \delta_K^v[J_z^2, J_{xy}^2]_+ - 2\delta_J^v J^2 J_{xy}^2 + H_K^v J_z^6 + H_{KJ}^v J_z^4 J^2 \\
&\quad + H_{JK}^v J_z^2 J^4 + H_J^v J^6 + [h_K^v J_z^4 + h_{JK}^v J_z^2 J^2 \\
&\quad + h_J^v J^4, J_{xy}^2]_+ + L_K^v J_z^8 + L_{KKJ}^v J_z^6 J^2 + L_{JK}^v J_z^4 J^4 \\
&\quad + L_{JJK}^v J_z^2 J^6 + L_J^v J^8 + [l_K^v J_z^6 + l_{KJ}^v J_z^4 J^2 + l_{JK}^v J_z^2 J^4 \\
&\quad + l_J^v J^6, J_{xy}^2]_+ + P_K^v J_z^{10} + P_{KKJ}^v J_z^8 J^2 + P_{KJ}^v J_z^6 J^4 \\
&\quad + P_{JK}^v J_z^4 J^6 + \cdots + S_K^v J_z^{12} + S_{KKJ}^v J_z^{10} J^2 + \cdots,
\end{aligned}
\tag{2}
$$

where J_α ($\alpha = x, y, z$) are the components of the angular momentum operator defined in the molecule-fixed coordinate system, $J_{xy}^2 = J_x^2 - J_y^2$, and $[\ldots, \ldots]_+$ denotes the anticommutator. Because of the symmetry arguments of the SO_2 molecule, the nondiagonal block operators can only be of two types: Coriolis interactions of the B_1 symmetry and Fermi interactions.

In our present study we follow the papers [26] and [31], where the bands $3\nu_3$ and $2\nu_1 + \nu_3$ have been discussed. This is the reason why only the Fermi-type interaction with the operator $|003\rangle\langle131|F^{003\,131}$ is taken into account in Equation (1).

4. Experimental spectrum and re-analysis of the bands $3\nu_3$ and $2\nu_1 + \nu_3$

The low resolution experimental spectra in the studied regions are shown in the upper parts of Figures 1 and 2 (to illustrate the quality of the experiment, the upper parts of Figures 3 and 4 present small fragments of the high resolution spectra). The absorption in both regions is provided by the relatively strong bands, $3\nu_3$ and $2\nu_1 + \nu_3$. As a result, it is practically impossible to recognise lines belonging to the considerably weaker bands, $\nu_2 + 3\nu_3 - \nu_2$ and $2\nu_1 + \nu_2 + \nu_3 - \nu_2$. To solve the problem of assigning the transitions of the hot bands, we made first a complete analysis of the rotational–vibrational structures of the bands $3\nu_3$ and $2\nu_1 + \nu_3$. As a result, we were able to

(a) assign about 2200 and 2300 transitions (more than 820 and 950 upper energy levels) with the maximum values of quantum numbers $J^{\text{max.}} = 60$, $K_a^{\text{max.}} = 19$, and $J^{\text{max.}} = 69$, $K_a^{\text{max.}} = 20$ for the bands $3\nu_3$ and $2\nu_1 + \nu_3$, respectively (in this case, the information about the ground vibrational state has been taken from [33]), and

(b) improve the spectroscopic parameters of the states (003) [26], and (201) [31]. It should be mentioned that the number of transitions obtained in [26] was 760, and the number of energy terms obtained in [31] was 499; in this case, the maximum values of quantum numbers $J^{\text{max.}} = 49$, $K_a^{\text{max.}} = 19$, and $J^{\text{max.}} = 53$, $K_a^{\text{max.}} = 16$ for the bands $3\nu_3$ and $2\nu_1 + \nu_3$, respectively, were achieved in [26] and [31].

The results of the fit of the assigned experimental transitions both for the $3\nu_3$, and $2\nu_1 + \nu_3$ bands are presented in Table 1 (columns 2 and 4) in comparison with the data from [26] and [31]. As can be seen, a good correlation exists between the two sets of data. In this case, the *rms*-deviation for the initially used line positions is 0.00025 cm^{-1}, that is close to the experimental uncertainties.

5. Analysis of the hot bands, $\nu_2 + 3\nu_3 - \nu_2$ and $2\nu_1 + \nu_2 + \nu_3 - \nu_2$

In the next step of our study, we simulated spectra corresponding to both bands, $3\nu_3$ and $2\nu_1 + \nu_3$.
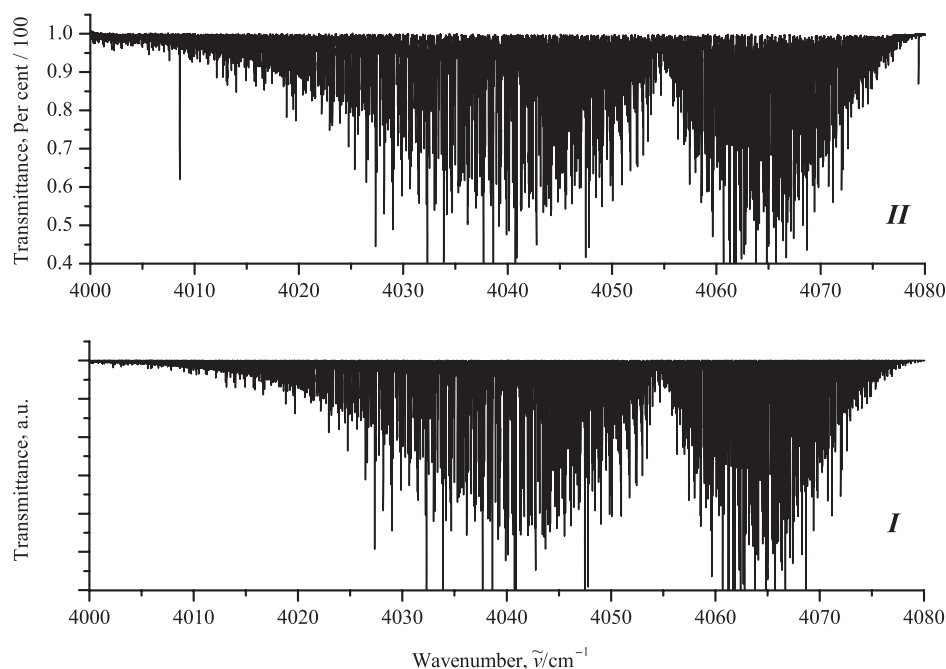
Figure 1. Survey spectrum of SO_2 in the region of the band $3\nu_3$: curves I and II are the simulated and the experimentally recorded spectra, respectively.
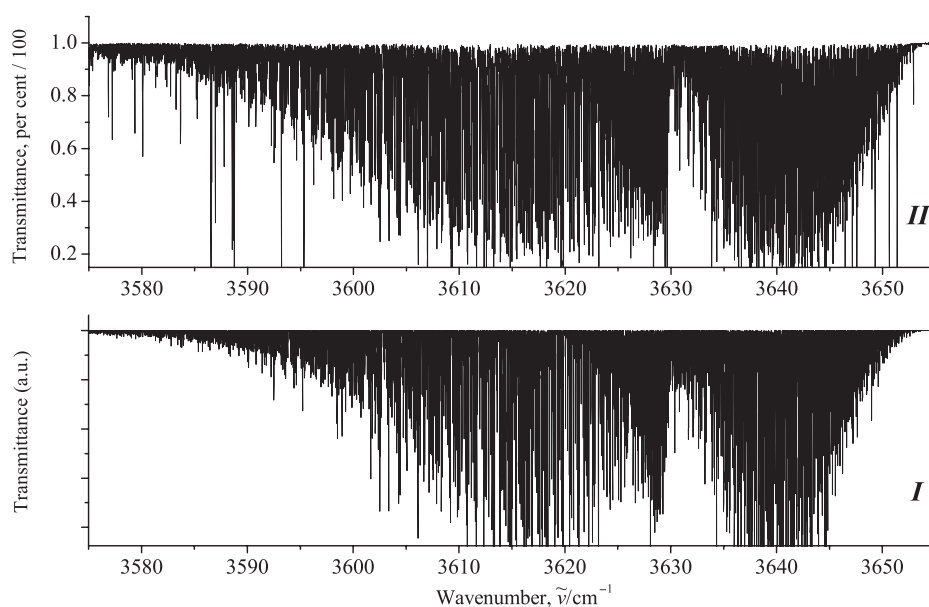
Figure 2. Survey spectrum of SO_2 in the region of the band $2\nu_1 + \nu_3$: curves I and II are the simulated and the experimentally recorded spectra, respectively.

The parameters obtained in the previous section were used to calculate the line positions; the relative line strengths were estimated in accordance with the general formulas from [42]. In this case, the dipole moment parameters from [1] and [31] were used to estimate the line strengths. As an illustration, the

simulated low resolution spectra and small parts of the high resolution simulations are shown on Figures 1–4, curves I. A good correspondence between the simulated and the experimental spectra is evident.

The experimental and simulated spectra were then compared, and the experimental spectrum was filtered

Figure 3. Small portion of the high resolution spectrum of the SO_2 molecule in the region of the P-branch of the $3\nu_3$ absorption band: curve II experimentally recorded spectrum; curve I simulated spectrum. The same dipole moment parameters were used in the simulation of both the cold, $3\nu_3$, and hot, $\nu_2 + 3\nu_3 - \nu_2$, bands. The dark squares denote transitions of the $3\nu_3$ band while the lines marked by dark triangles belong to the $\nu_2 + 3\nu_3 - \nu_2$ band.

by taking the lines belonging to the 'cold' bands, $3\nu_3$ and $2\nu_1 + \nu_3$. We believe that most of the remaining lines belong to the 'hot' bands, $\nu_2 + 3\nu_3 - \nu_2$ and $2\nu_1 + \nu_2 + \nu_3 - \nu_2$.

We point out that after this procedure, only very weak lines can be seen in the filtered experimental spectrum. Moreover, due to the weakness of the transitions, it is virtually impossible to find sets of them connected by ground state combination differences, and therefore, an assignment by traditional methods cannot be carried out. However, we can use the potential function of the SO_2 molecule from [37] that allows us to predict with a satisfactory accuracy the values of both the band centres, and the main rotational parameters of the studied vibrational states (013) and (211). In this case, one can expect that such a calculation will determine the values of the rotational energy spacings within a given vibrational state much better than the values of the band centres. This is due to the fact (see [37]) that the rotational energy spacings for the states with the value of the quantum number $J \leq 4$ are reproduced by the potential parameters from [37] with an accuracy about 300 times better than the values of the band centres. Thus, we have calculated the transitions in the 'hot' bands, $\nu_2 + 3\nu_3 - \nu_2$ and $2\nu_1 + \nu_2 + \nu_3 - \nu_2$, and we have estimated that the accuracy of the spacings between line positions

within one band is generally better than 0.04–0.05 cm^{-1} for the transitions with $J^{\text{upper}} \leq 6$–8.

We have then varied the vibrational energies and the rotational parameters, A and B, of the states (013) and (211) with steps of 0.005, 0.0005, and 0.0005 cm^{-1}, respectively. For each value of the vibrational energy and of the A and B parameters we obtained the number N of experimental transition wavenumbers that coincided with the calculated ones to 0.005 cm^{-1} or better. The results of this analysis are shown in Figures 5 and 6 where we plot N against the vibrational term value for $\nu_2 + 3\nu_3 - \nu_2$ and $2\nu_1 + \nu_2 + \nu_3 - \nu_2$, respectively. In each case there is a particular value of the vibrational term value for which N has a distinct maximum. We would like to emphasise that Figure 6 presents a plot of N against the value of the vibrational energy for the optimal values of the rotational parameters A and B (in reality, all three parameters were varied simultaneously) for the $2\nu_1 + \nu_2 + \nu_3 - \nu_2$ band. Figure 5 presents analogous plots for the $\nu_2 + 3\nu_3 - \nu_2$ band. To illustrate the dynamics of change of the value N, plots curves I, II and III of Figure 5 correspond to the same optimal value of the B parameter, but the values of the A parameter are different: $A = A^{\text{opt.}}$ for curve III; $A = A^{\text{opt.}} + 0.0015$ cm^{-1} and $A = A^{\text{opt.}} + 0.0030$ cm^{-1} for the curves II and I, respectively.

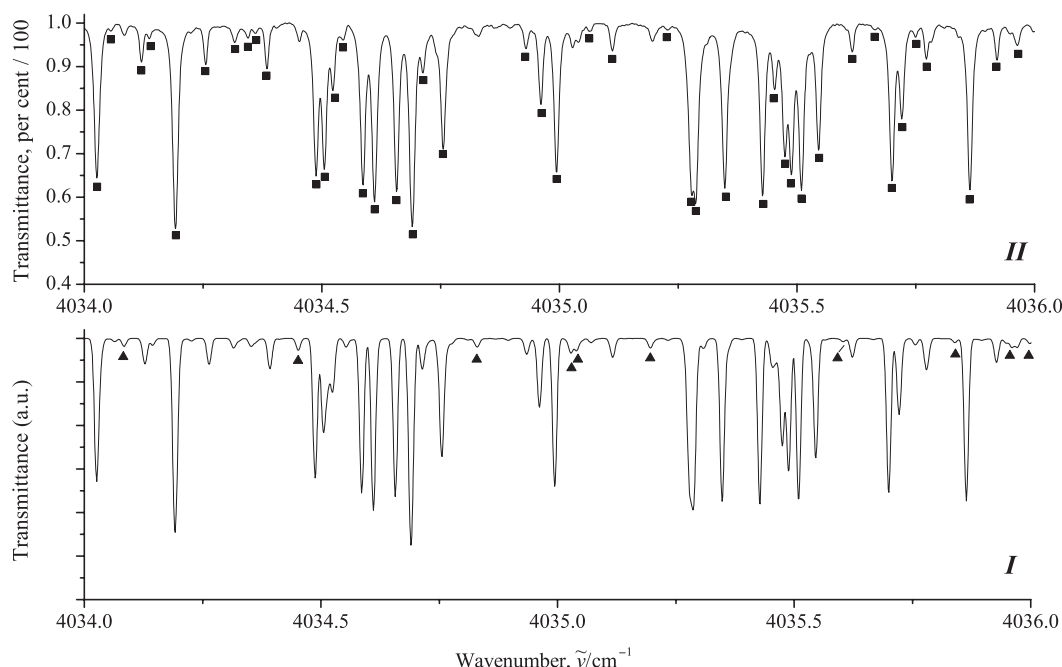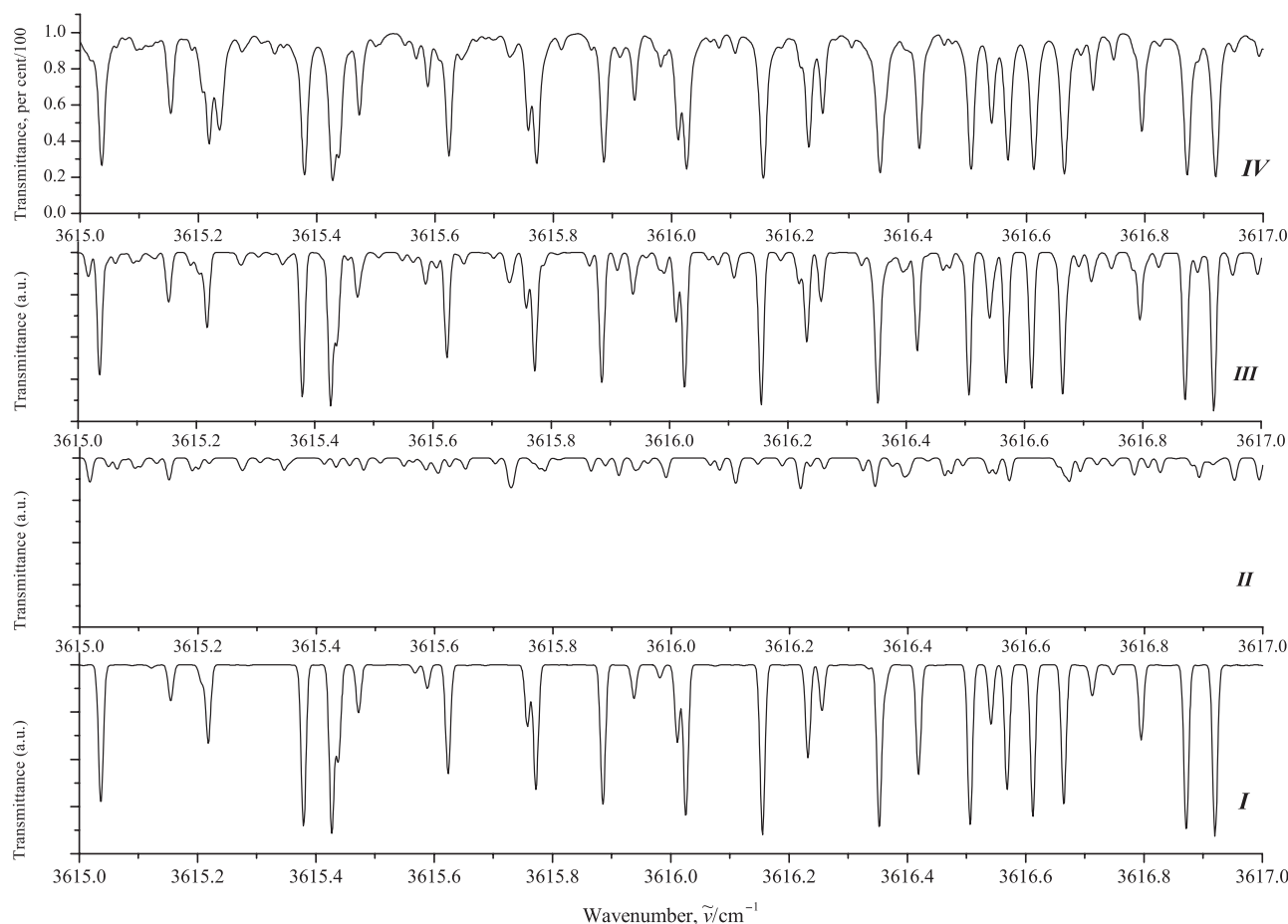Figure 4. Small portion of the high resolution spectrum of the SO_2 molecule in the region of the $2\nu_1 + \nu_3$ absorption band: curve IV is the experimentally recorded spectrum, and the three lower traces (curves I–III) present simulated spectra. The traces of curves I and II show the lines belonging to the 'cold' band, $2\nu_1 + \nu_3$, and the 'hot' band, $2\nu_1 + \nu_2 + \nu_3 - \nu_2$, respectively. The sum of the simulated spectra curves I and II is given by the trace of curve III.

At the final step of the analysis, the transitions obtained with the above procedure were used as initial data in the fit with the Hamiltonian model of an isolated vibrational state, Equation (2). Then, the improved rotational and centrifugal distortion parameters were used in the search for additional transitions of the bands $\nu_2 + 3\nu_3 - \nu_2$ and $2\nu_1 + \nu_2 + \nu_3 - \nu_2$, and a second fit was performed. Results of the final fit are shown in the columns 2 and 4 of Table 2, together with their 1σ statistical confidence intervals. The values of parameters that are given in columns 2 and 4 without confidence intervals were constrained to the values from columns 3 and 5, respectively. The values of the parameters A, B, and C in columns 3 and 5 have been estimated in two different ways: (a) on the basis of rotation–vibration α-coefficients from [26], and (b) on the basis of parameters of the intramolecular potential function from [37]. As expected, both sets of estimated values proved to be quite close to each other.

The vibrational energies E were predicted using the parameters of the potential function from [37]. The values of all centrifugal distortion coefficients were also estimated from the known values of the corresponding parameters of the ground vibrational state and of the state (010) from [33], and of the states (003) [26], and (201) [31].

In general, the 230 and the 115 transitions that have been assigned respectively to the bands $\nu_2 + 3\nu_3 - \nu_2$ and $2\nu_1 + \nu_2 + \nu_3 - \nu_2$ (the list of assigned transitions is available in the electronic supplementary data[1]), are reproduced with a *rms*-deviation of $0.00059 \, \text{cm}^{-1}$ which is comparable with the uncertainties of weak lines in the experimental spectrum. To illustrate the quality of the results, Figure 3, curve I and Figure 4, curve III give some small parts of the simulated spectra for the regions of the $\nu_2 + 3\nu_3 - \nu_2$ and $2\nu_1 + \nu_2 + \nu_3 - \nu_2$ bands. One can see a good line-by-line correlation between the simulated spectra

Table 1. Spectroscopic parameters of the (201), (003), and (131) vibrational states of the SO_2 molecule (in cm^{-1}).

Parameter	$(201)^a$	$(201)^b$	$(003)^a$	$(003)^c$	$(131)^c$
1	2	3	4	5	6
E	3629.761502 (90)	3629.761938	4054.000928 (10)	4054.0011	4029.3903
A	2.00830905 (13)	2.008300210	1.96601132 (13)	1.966002305	2.129711
B	0.339697900 (31)	0.3396993164	0.340668901 (14)	0.340668827	0.3415573
C	0.289554048 (18)	0.2895536306	0.2902511765 (99)	0.2902507916	0.2893848
$\Delta_K \times 10^5$	8.764045 (31)	8.7598413	8.24718 (10)	8.2406848	11.54
$\Delta_{JK} \times 10^6$	−3.889663 (64)	−3.8884712	−4.367556 (33)	−4.36800817	−4.46
$\Delta_J \times 10^7$	2.219278 (60)	2.2198220	2.285216 (31)	2.2840366	2.23
$\delta_K \times 10^7$	9.6303 (92)	9.468801	6.7975 (22)	6.86892	12.8
$\delta_J \times 10^8$	5.69687 (32)	5.711601	5.88911 (21)	5.891628	5.85
$H_K \times 10^8$	1.290963	1.290963	1.15448 (20)	1.1417121	2.17
$H_{KJ} \times 10^{10}$	−6.7161	−6.7161	−4.66421	−4.66421	−9.88
$H_{JK} \times 10^{12}$	1.3250	1.3250	1.3250	1.3250	1.3250
$H_J \times 10^{13}$	4.0672	4.0672	5.1477	5.1477	1.99
$h_K \times 10^{10}$	5.7057	5.7057	5.3318	5.3318	9.0
$h_{JK} \times 10^{13}$	−3.78565	−3.78565	−3.7865	−3.7865	−39.8
$h_J \times 10^{13}$	1.4878	1.4878	2.1	2.1	2.08
$L_K \times 10^{12}$	−2.76650	−2.76650	−2.69	−2.69	−5.06
$L_{KKJ} \times 10^{13}$	1.44532	1.44532	1.44532	1.44532	
$L_{JK} \times 10^{16}$	7.728	7.728	7.728	7.728	
$L_{JJK} \times 10^{16}$	−1.2014	−1.2014	−1.2014	−1.2014	
$L_J \times 10^{18}$	−3.099	−3.099	−3.099	−3.099	
$P_K \times 10^{16}$	7.4675	7.4675	7.4675	7.4675	
$P_{KKJ} \times 10^{17}$	−2.6122	−2.6122	−2.6122	−2.6122	
$F^{003-131} \times 10^2$			3.301153	3.301153	

Notes: ^{a}Values in parentheses are 1σ statistical confidence intervals (in last digits). Parameters presented without confidence intervals were constrained to the values of corresponding parameters from [31] and [26] (see, columns 3 and 5).
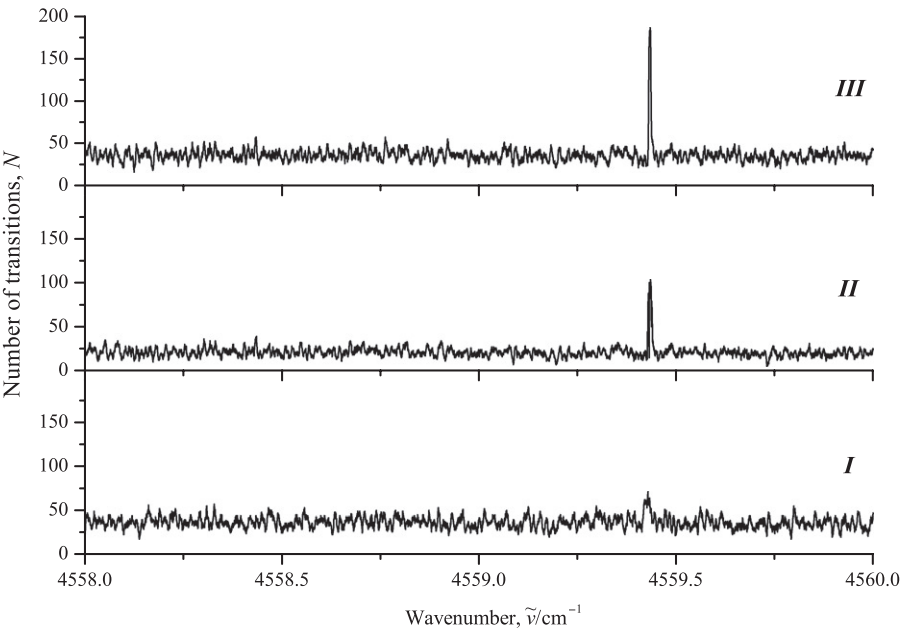^{b}Reproduced from [31].
^{c}Reproduced from [26].

Figure 5. The number N of observed lines that coincide with calculated lines to within $0.005\,cm^{-1}$ for the $\nu_2 + 3\nu_3 - \nu_2$ hot band of SO_2 plotted as a function of the theoretical vibrational energy. The plots curves I–III correspond to different values of the rotational parameter A (see text).
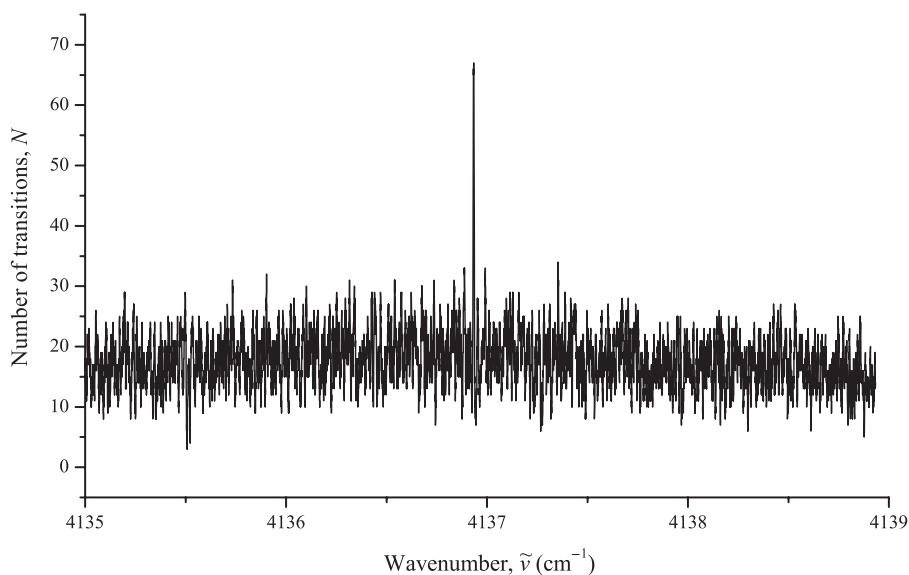
Figure 6. The number N of observed lines that coincide with calculated lines to within $0.005\,\mathrm{cm}^{-1}$ for the $2\nu_1+\nu_2+\nu_3-\nu_2$ hot band of SO_2 plotted as a function of the theoretical vibrational energy.

Table 2. Spectroscopic parameters of the (211) and (013) vibrational states of the SO_2 molecule (in cm^{-1}).

Parameter	$(211)^a$	$(211)^b$	$(013)^a$	$(013)^b$
1	2	3	4	5
E	4136.93408 (39)	4137.32	4559.434000 (18)	4559.29
A	2.0474072 (19)	2.04748	2.00350754 (87)	2.00518
B	0.3397914 (20)	0.33945	0.34073038 (14)	0.34042
C	0.2890258 (26)	0.28929	0.28967810 (13)	0.28998
$\Delta_K \times 10^5$	9.7223 (25)	9.705	9.11796 (84)	9.188
$\Delta_{JK} \times 10^6$	−4.0222 (43)	−4.060	−4.52949 (92)	−4.538
$\Delta_J \times 10^7$	2.224	2.224	2.28524 (77)	2.290
$\delta_K \times 10^7$	11.530	11.530	8.116 (63)	8.687
$\delta_J \times 10^8$	5.731	5.731	5.9285 (66)	5.922
$H_K \times 10^8$	1.587	1.587	1.450	1.450
$H_{KJ} \times 10^{10}$	−7.792	−7.792	−5.740	−5.740
$H_{JK} \times 10^{12}$	4.737	4.737	4.737	4.737
$H_J \times 10^{13}$	4.054	4.054	5.135	5.135
$h_K \times 10^{10}$	7.646	7.646	7.272	7.272
$h_{JK} \times 10^{13}$	−9.196	−9.196	−9.196	−9.196
$h_J \times 10^{13}$	1.491	1.491	2.100	2.100
$L_K \times 10^{12}$	−3.838	−3.838	−3.762	−3.762
$L_{KKJ} \times 10^{13}$	2.028	2.028	2.028	2.028
$L_{JK} \times 10^{15}$	−3.754	−3.754	−3.754	−3.754
$L_{JJK} \times 10^{16}$	−1.517	−1.517	−1.517	−1.517
$L_J \times 10^{18}$	−2.999	−2.999	−2.999	−2.999
$P_K \times 10^{15}$	1.144	1.144	1.144	1.144
$P_{KKJ} \times 10^{17}$	−4.559	−4.559	−4.559	−4.559

Notes: [a]Values in parentheses are 1σ statistical confidence intervals (in last digits). Parameters presented without confidence intervals were constrained to predicted values from columns 3 and 5, respectively. [b]Constrained to the predicted values (see text for details).

and the experimental ones presented on Figure 3, curve II and Figure 4, curve IV.

6. Conclusion

We have presented the first high resolution analysis of the very weak hot bands, $\nu_2 + 3\nu_3 - \nu_2$ and $2\nu_1 + \nu_2 + \nu_3 - \nu_2$. Our analysis is based on a variational procedure that allowed us to assign, respectively, 230 and 115 transitions to the above-mentioned bands. The spectroscopic parameters for the highly excited vibrational states, (013) and (211), reproduce the corresponding line positions with a *rms*-deviation of $0.00059\,\mathrm{cm}^{-1}$. The variational procedure used here demonstrates a high efficiency and, we believe, can also be applied to study of weak bands of other polyatomic molecules.

Acknowledgements

Note

1. The supplementary data can be viewed online.

References

[1] W.J. Lafferty, G.T. Fraser, A.S. Pine, J.-M. Flaud, C. Camy-Peyret, V. Dana, J.-Y. Mandin, A. Barbe, J.J. Plateaux, and S. Bouazza, J. Mol. Spectrosc. **154**, 51 (1992).

[2] P.M. Chu, S.J. Wetzel, W.J. Lafferty, A. Perrin, J.-M. Flaud, Ph. Arcas, and G. Guelachvili, J. Mol. Spectrosc. **189**, 55 (1998).

[3] A.J. Lovas, J. Phys. Chem. Ref. Data **14**, 395 (1985).

[4] E.D. Hinkley, A.R. Calawa, P.J. Kelley, and S.A. Clough, J. Appl. Phys. **43**, 3222 (1972).

[5] G.D. Tejwani, J. Chem. Phys. **57**, 4676 (1972).

[6] W.H. Yang, J.A. Roberts, and G.D. Tejwani, J. Chem. Phys. **58**, 4916 (1973).

[7] M. Carlotti, G. DiLonardo, L. Fusina, È. Carli, and F. Mencaraglia, J. Mol. Spectrosc. **106**, 235 (1984).

[8] P.A. Helminger and F.C. DeLuchia, J. Mol. Spectrosc. **111**, 66 (1985).

[9] A. Barbe, C. Secroun, P. Jouve, B. Duterage, N. Monnanteuil, J. Bellet, and G. Steenbeckeliers, J. Mol. Spectrosc. **55**, 319 (1975).

[10] G. Steenbeckeliers and J. Bellet, J. Appl. Phys. **46**, 2620 (1975).

[11] P.J. Pilon and C. Young, J. Quant. Spectrosc. Radiat. Transfer **16**, 1137 (1976).

[12] A. Barbe, C. Secroun, P. Jouve, B. Duterage, N. Monnanteuil, and J. Bellet, Mol. Phys. **34**, 127 (1977).

[13] A.S. Pine and P.F. Moulton, J. Mol. Spectrosc. **64**, 15 (1977).

[14] A.S. Pine, G. Dresselhaus, B. Palm, R.W. Davies, and S.A. Clough, J. Mol. Spectrosc. **67**, 386 (1977).

[15] N.I. Moskalenko, V.F. Terzi, S.N. Parzhin, V.T. Pushkin, and R.S. Sadydov, Izv. Acad. Sci. USSR, Atmos. Oceanic Phys. **14**, 901 (1978).

[16] F. Herlemont, M. Lyszyk, and J. Lemaire, J. Mol. Spectrosc. **77**, 69 (1979).

[17] J.P. Satler, T.L. Worchesky, and W.J. Lafferty, J. Mol. Spectrosc. **77**, 364 (1981).

[18] T. Kunitomo, H. Masuzaki, S. Ueoka, and M. Osumi, J. Quant. Spectrosc. Radiat. Transfer **25**, 345 (1981).

[19] K. Kim and W.T. King, J. Chem. Phys. **80**, 969 (1984).

[20] F. Kuhnemann, Y. Heiner, B. Sumpf, and K. Hermann, J. Mol. Spectrosc. **152**, 1 (1992).

[21] G. Guelachvili, O.N. Ulenikov, and G.A. Ushakova, J. Mol. Spectrosc. **108**, 1 (1984).

[22] G. Guelachvili, O.V. Naumenko, and O.N. Ulenikov, Appl. Opt. **23**, 2862 (1984).

[23] G. Guelachvili, O.V. Naumenko, and O.N. Ulenikov, J. Mol. Spectrosc. **125**, 128 (1987).

[24] J.-M. Flaud, A. Perrin, L.M. Salah, W.J. Lafferty, and G. Guelachvili, J. Mol. Spectrosc. **160**, 272 (1993).

[25] L. Coudert, A.G. Maki, and Wm.B. Olson, J. Mol. Spectrosc. **124**, 437 (1987).

[26] J.-M. Flaud and W.J. Lafferty, J. Mol. Spectrosc. **161**, 396 (1993).

[27] W.J. Lafferty, A.S. Pine, J.-M. Flaud, and C. Camy-Peyret, J. Mol. Spectrosc. **157**, 499 (1993).

[28] B. Sumpf, O. Fleischmann, and H.D. Kronfeldt, J. Mol. Spectrosc. **176**, 127 (1996).

[29] B. Sumpf, M. Schone, and H.D. Kronfeldt, J. Mol. Spectrosc. **179**, 137 (1996).

[30] S.P. Belov, M.Y. Tretyakov, I.N. Kozin, E. Klisch, G. Winnewisser, W.J. Lafferty, and J.-M. Flaud, J. Mol. Spectrosc. **191**, 17 (1998).

[31] W.J. Lafferty, A.S. Pine, G. Hilpert, R.L. Sams, and J.-M. Flaud, J. Mol. Spectrosc. **176**, 280 (1996).

[32] W.J. Lafferty, J.-M. Flaud, and G. Guelachvili, J. Mol. Spectrosc. **188**, 106 (1998).

[33] H.S.P. Müller and S. Brünken, J. Mol. Spectrosc. **232**, 213 (2005).

[34] W.J. Lafferty, J.-M. Flaud, R.L. Sams, and El Hadji Abib Ngom, J. Mol. Spectrosc. **252**, 72 (2008).

[35] W.J. Lafferty, J.-M. Flaud, El Hadji Abib Ngom, and R.L. Sams, J. Mol. Spectrosc. **253**, 51 (2009).

[36] O.N. Ulenikov, E.S. Bekhtereva, V.-M. Horneman, S. Alanko, and O.V. Gromova, J. Mol. Spectrosc. **255**, 111 (2009).

[37] O.N. Ulenikov, E.S. Bekhtereva, V.-M. Horneman, S. Alanko, O.V. Gromova, and C. Leroy, J. Mol. Spectrosc. **257**, 137 (2009).

[38] T. Ahonen, S. Alanko, V.-M. Horneman, M. Koivusaari, R. Paso, A.-M. Tolonen, and R. Anttila, J. Mol. Spectrosc. **181**, 279 (1997).

[39] R.A. Toth, J. Opt. Soc. AM. B **10**, 2006 (1993).

[40] V.-M. Horneman, Thesis, Acta Univ. Oulu **A 321**, 127 (1992).

[41] J.K.G. Watson, J. Chem. Phys. **46**, 1935 (1967).

[42] J.-M. Flaud and C. Camy-Peyret, J. Mol. Spectrosc. **55**, 278 (1975).